Orbital fluctuating state in ferromagnetic insulating $LaMnO_{3+\delta}$ ($0.085 \leqslant \delta \leqslant 0.125$) studied using Raman spectroscopy

K.-Y. Choi,[1] Yu. G. Pashkevich,[2] V. P. Gnezdilov,[3] G. Güntherodt,[4] A. V. Yeremenko,[3] D. A. Nabok,[2] V. I. Kamenev,[2] S. N. Barilo,[5] S. V. Shiryaev,[5] A. G. Soldatov,[5] and P. Lemmens[6]

[1]*Institute for Materials Research, Tohoku University, Katahira 2-1-1, Sendai 980-8577, Japan*

[2]*A. A. Galkin Donetsk Phystech NASU, 83114 Donetsk, Ukraine*

[3]*B. I. Verkin Institute for Low Temperature Physics NASU, 61164 Kharkov, Ukraine*

[4]*2. Physikalisches Institut, RWTH Aachen, 52056 Aachen, Germany*

[5]*Institute of Physics of Solids & Semiconductors, Academy of Sciences, 220072 Minsk, Belarus*

[6]*Institute for Physics of Condensed Matter, TU Braunschweig, D-38106 Braunschweig, Germany*

(Received 8 April 2006; revised manuscript received 24 June 2006; published 10 August 2006)

A giant softening by 30 cm^{-1} of the 490 and 620 cm^{-1} Jahn-Teller and breathing optical phonon modes is observed in Raman spectroscopy below the Curie temperature of single crystalline $LaMnO_{3+\delta}$ ($0.085 \leqslant \delta \leqslant 0.125$). A pseudogaplike suppression of a continuum and a Fano antiresonance at 144 cm^{-1} appear below the charge-ordering temperature. Upon going through the antiferromagnetic/ferromagnetic insulating phase boundary a high-frequency maximum of three-peaks structure evolves to a unstructured, broadened maximum while undergoing a softening in the peak energy. This is interpreted in terms of the presence of fluctuating orbitals and mobile holes which form a stripelike state in the lightly doped, insulating manganites.

DOI: 10.1103/PhysRevB.74.064406 PACS number(s): 75.50.Cc, 71.38.−k, 63.20.−e

I. INTRODUCTION

One topical issue in the physics of manganites is the role of orbital degrees of freedom as well as the state of the orbital subsystem at different doping levels in explaining the complex phase diagram.[1,2] The most intriguing feature is found in a ferromagnetic insulating (FMI) phase of the lightly doped $La_{1-x}Sr_xMnO_3$ ($x=0.11-0.17$).[3–12]

With lowering temperature the FMI samples exhibit cooperative Jahn-Teller (JT) distortions at T_{JT}. Upon further cooling a transition from a paramagnetic insulating (PI) to a ferromagnetic (FM) state takes place at T_C where the resistivity starts to decrease. Between T_{JT} and T_C a $d_{3x^2-r^2}/d_{3y^2-r^2}$ orbital ordering is present, which is similar to that of $LaMnO_3$.[9,10] Finally, with decreasing temperature the FM state undergoes a transition to a FMI state at T_{CO}, while the resistivity shows a sharp upturn. At the respective low temperatures, neutron and x-ray studies[5,7] show a superstructure interpreted in terms of long-range charge order. Recently, resonant x-ray scattering has proved the related formation of orbital polarons.[9–11] In addition, Raman scattering measurements have observed the giant softening of Mn-O stretching mode, interpreted in terms of fluctuating orbital state.[12] Further, there is considerable evidence for a structural modulation with alternating hole-poor and hole-rich planes along the *c* axis as well as a nonuniform charge distribution.[6,7,13,14] In spite of extensive studies, however, the full aspect of the orbital and charge correlations has not yet emerged because of the formation an inhomogeneous Mn subsystem where spin, orbital, and charge are closely coupled.

In this situation, a study of the nonstoichiometric counterpart $LaMnO_{3+\delta}$ ($0.071 \leqslant \delta \leqslant 0.125$) can provide new insight into this issue. This is because vacancies on Mn and La sites and the related disorder can disturb the delicate balance of a charge- and orbital-ordered state. In addition, the availability of detwinned single crystals enables us to extract more specific information, which is not possible in twinned $La_{1-x}Sr_xMnO_3$ samples.

The structural and magnetic properties of the studied samples are summarized in Table I. Our results are consistent with previous studies.[15,16] As δ increases, a distorted orthorhombic O′ phase ($\delta=0.071-0.085$) transits to a pseudocubic one ($\delta=0.092-0.096$) and then to a rhombohedral one ($\delta=0.096-0.125$). This implies a systematic reduction of the distortions of the MnO_6 octahedra by changing continuously the Mn^{4+}/Mn^{3+} ratio in a wide range. For the ferromagnetic samples ($0.085 \leqslant \delta \leqslant 0.125$) the magnetization shows a steplike jump at T_C and T_{CO}.[17] The overall behavior is quite similar to the lightly doped $La_{1-x}Sr_xMnO_3$ ($0.11 \leqslant x \leqslant 0.15$) (compare Refs. 10 and 17). This tells us that the crystal symmetry is reduced to triclinic for temperatures below T_{CO} as observed in the $La_{1-x}Sr_xMnO_3$ compounds.[9,10] However, there also appear some discrepancies;[17] (i) the irreversibility in the field-cooled and zero-field cooled magnetization, and (ii) the drop of magnetization under zero-field cooling for low temperatures below T_{CO}. This might be related to additional cation vacancies leading to the metastability of the charge- and orbital-ordered state.

We report Raman scattering measurements on the lightly oxygen-doped manganites $LaMnO_{3+\delta}$. A giant and continuous softening of Mn-O bond stretching modes below the Curie temperature and an unstructured, broadened multiphonon feature suggest a fluctuating orbital state in FMI samples ($0.085 \leqslant \delta \leqslant 0.125$). A pseudogaplike electronic response below the charge-ordering temperature together with a Fano antiresonance at 144 cm^{-1} signals the significance of hole mobilities in the charge-ordered background. This is ascribed to a formation of a stripelike state of holes.

II. EXPERIMENTAL DETAILS

$LaMnO_{3+\delta}$ single crystals were grown by using a modified method of McCarrol *et al.*,[18] which allows for doping without inducing a large cation mass difference and related

TABLE I. Structural and magnetic properties of $LaMnO_{3+\delta}$ with O ($c \leqslant b/\sqrt{2} < a$) and O′ ($b/\sqrt{2} < c < a$) orthorhombic phases with *Pnma* space-group symmetry and *R* a rhombohedral phase with $R\bar{3}c$ space-group symmetry.

Sample $3+\delta$	Charge ordering	Magnetic ordering	V/f.u. (Å^3) $T=300$ K	Lattice parameters	Crystal structure
3.071		$T_N=128$ *K*	59.73	$a=5.529$, $b=5.572$, $c=7.756$	O′
3.085	$T_{CO}=131$ *K*	$T_C=148$ *K*	59.54	$a=5.524$, $b=5.549$, $c=7.770$	O′
3.092	$T_{CO}=146$ *K*	$T_C=178$ *K*	59.45	$a=5.493$, $b=5.536$, $c=7.821$	O
3.096	$T_{CO}=152$ *K*	$T_C=186$ *K*	59.41	$a=5.493$, $b=5.537$, $c=7.818$	O
3.125		$T_C=248$ *K*	59.06	$a=3.894$, $\alpha=90.56$	*R*

disorder and effects of clustering. The samples are detwinned. The true crystallographic formula corresponds to $La_{1-x}Mn_{1-y}O_3$ with $3/2(x+y) \approx \delta$. Cation vacancies were controlled by varying the melting temperature. Samples were characterized by x-ray diffraction, magnetic susceptibility, and chemical analysis as summarized in Table I.

Raman scattering experiments were performed using the excitation line $\lambda=514.5$ nm of an Ar^+ laser in a quasiback-scattering geometry. The laser power of 5 mW was focused to a 0.1 mm diameter spot on the (010) surface. The scattered spectra were collected by a DILOR-XY triple spectrometer and a nitrogen cooled charge-coupled device detector.

III. RESULTS AND DISCUSSIONS

Figure 1 displays the doping dependence of Raman spectra of $LaMnO_{3+\delta}$ ($\delta=0.071$, 0.085, 0.092, 0.096, and 0.125) in ($x'x'$) polarization at 5 and 295 K, respectively. The data are compared to lightly doped manganites $La_{1-x}Sr_xMnO_3$ ($x=0.06$, 0.11, 0.125, and 0.14) that are the counterpart to the title compound.[12] Remarkably, the observed Raman spectra resemble each other. The antiferromagnetic (AFI) samples ($\delta=0.071$ and $x=0.06$) show weak peaks arising from vibrations of (La/Sr) cations and rotations of the MnO_6 octahedra in addition to the three main peaks: the out-of-phase rotational mode around 250 cm^{-1}, the JT mode around 490 cm^{-1}, and the breathing mode around 620 cm^{-1}. No drastic temperature dependence is observed. In contrast, at low temperature the FMI samples ($\delta=0.085-0.125$ and $x=0.11-0.14$) exhibit extra phonon peaks, which are split off from the high-temperature modes. Since the crystal symmetry is lowered due to the orbital rearrangements at T_{CO},[10] the extra phonon modes might arise from the symmetry reduction. In this case, activated modes are expected to be weak. However, the observed modes are sharp as well as intense. Moreover, they show up as a shoulder of the high-temperature

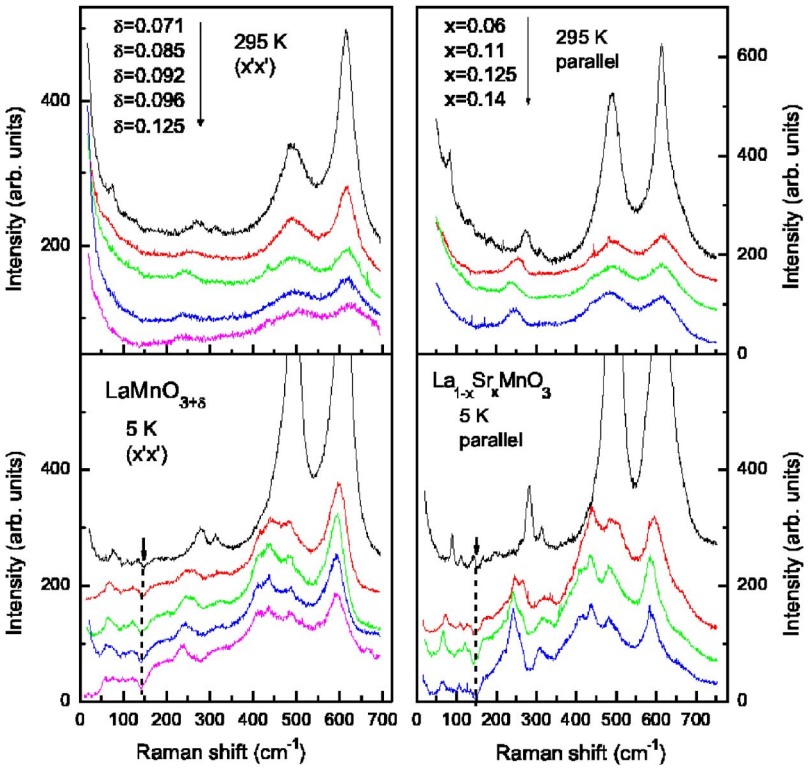

FIG. 1. (Color online) (Left panels) Raman spectra of $LaMnO_{3+\delta}$ ($\delta=0.071$, 0.085, 0.092, 0.096, and 0.125) in ($x'x'$) polarization as a function of doping at 5 and 295 K, respectively. (Right panels) For comparison, Raman spectra of $La_{1-x}Sr_xMnO_3$ ($x=0.06$, 0.11, 0.125, and 0.14) are presented together at the respective temperature (Ref. 12).

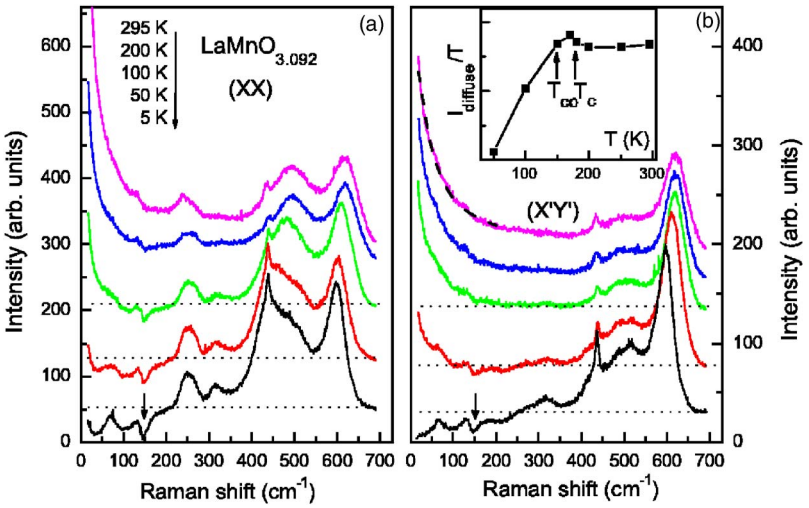

FIG. 2. (Color online) Temperature dependence of Raman spectra of $LaMnO_{3+\delta}$ (δ=0.092) in (a) (xx) and (b) ($x'y'$) polarizations. The horizontal dotted lines are a guide to the eye to emphasize the electronic background. The vertical arrows indicate the antiresonance at 144 cm^{-1}. The dashed line on Raman spectrum at 295 K represents a fitting of the low-frequency electronic response using a diffusive scattering formula (see the text). Inset: The inset gives the normalized scattering amplitude, I_{diff}/T.

modes. This suggests that most of them are zone-folded modes induced by the charge ordering and orbital ordering.

Noticeably, all FMI samples have identical Raman spectra, irrespective of doping and composition. This implies that all FMI samples are characterized by the same charge- and orbital-ordering structure in spite of additional, disordered holes as well as of chemical disorder induced by doping. This is substantiated by (i) x-ray measurements of $La_{1-x}Sr_xMnO_3$, which exhibits the same superstructure reflections of nearly equal scattering intensity for all x[5] and (ii) a resonant x-ray scattering study that uncovers the forbidden reflection induced by an orbital rearrangement at the same position for all x.[19]

Shown in Fig. 2 is the temperature dependence of the Raman spectra of a representative sample with δ=0.092 in (xx) and ($x'y'$) polarizations. These data have several intriguing features. With decreasing temperature the Mn-O stretching modes undergo a large softening and new phonon peaks show up. Furthermore, the low-frequency quasielastic response exhibits a substantial redistribution of spectral weight as a function of temperature. Significantly, a strong Fano antiresonance is observed at the 144 cm^{-1} mode, which corresponds to the mixed vibrations of the La and O1 atoms in the xz plane.[20] As shown in Ref. 21, a ferro-orbital ordering along the c axis is favored when all O1 ions push the La ion in the same direction. On the other hand, an antiferro-orbital ordering is stabilized when the O1 ions between the upper and lower plane push the La ion in the opposite direction. This implies that an orbital ordering forms along the c axis and this ordering is characterized by the type of static distortion of the La and O1 ions. Thus, the 144 cm^{-1} mode is intrinsically coupled to the pattern of the orbital ordering. Since the antiresonance arises from electron-phonon coupling, the observed Fano antiresonance gives evidence for the presence of a continuum arising from orbital fluctuations between antiferro- to ferro-orbital ordering along the c axis.

We notice that the weak antiresonance is already present in the AFI sample and becomes stronger in the FMI samples (see the left lower panel of Fig. 1). This suggests that a ferromagnetic orbital droplet is formed in the antiferromagnetic orbital background. Upon going through the FMI phase, the ferromagnetic orbital state, composed of an orbital polaron, becomes predominant, while being in a fluctuating state.[9,10,12] This explains the strong antiresonance in the FMI samples. Hence, we conclude that holes are not totally frozen-in below T_{CO}, leading to orbital fluctuations via hole-orbital coupling.

To get more information on the evolution of hole dynamics we will inspect the electronic response. At high temperatures the observed quasielastic Raman response is well described by a diffusive scattering,[22]

$$I(\omega,T) = 1/[1-\exp(-\hbar\omega/kT)](I_{diff}\omega\Gamma)/(\omega^2+\Gamma^2).$$

Here the first term is the Bose-thermal factor, I_{diff} is the scattering amplitude, and Γ is the scattering rate. The dashed line represents a fit to the data at 295 K. The scattering rate of Γ=13.5–14.5 cm^{-1} is very small and hardly varies with temperature (not shown here). This is characteristic for a collision-dominated scattering of the insulating state. Note that its magnitude is two orders of magnitude smaller than that of the metallic $La_{1-x}Sr_xMnO_3$.[22] Since a scattering amplitude varies strongly with scattering channels, we plot the scattering amplitude divided by temperature, I_{diff}/T, in the inset of Fig. 2(b). Upon cooling, the I_{diff}/T shows a subtle but distinct upsurge between T_{CO} and T_C and then decreases rapidly. This feature evidences the presence of the diffusive scattering from orbitals since an orbital rearrangement occurs in the corresponding temperature interval. However, the small upsurge implies that orbital disorder is not significant through the reordering in the orbital sector. Therefore, the diffusive scattering might be governed by electronic scattering of spins. This is consistent with thermodynamic experiments that show a dominant magnetic contribution to the entropy change below T_C.[8]

At low temperatures the spectral weight of the diffusive scattering is suppressed for frequencies below 250 cm^{-1}. Such a behavior is typical for a pseudogap state in strongly correlated systems. Thus, our study provides spectroscopic evidence for the presence of a pseudogap state in the FMI state. We mention that it has been reported in a ferromagnet metallic state of the bilayer manganite $La_{1.2}Sr_{1.8}Mn_2O_7$.[23] Remarkably, similar electronic excitations have been observed in $La_{2-x}Sr_xNiO_4$ with a pronounced Fano

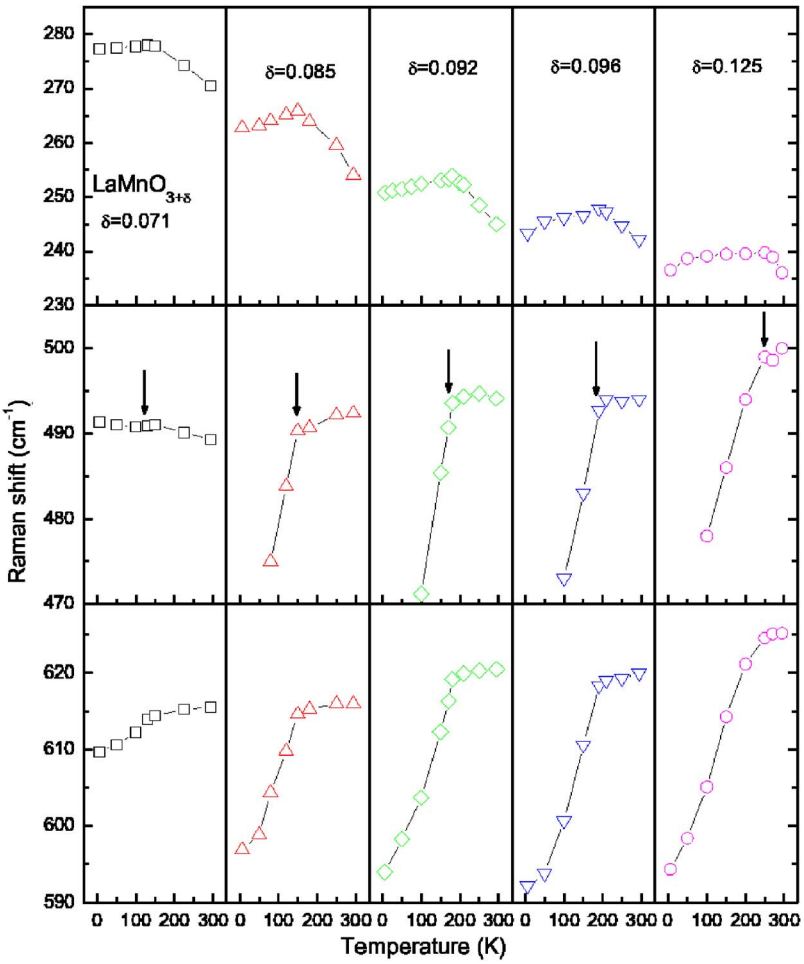

FIG. 3. (Color online) Temperature dependence of peak position of the 250, 490, and 620 cm^{-1} mode as a function of doping δ. The vertical arrows indicate the magnetic-ordering temperature.

antiresonance.[24] In the nickelates, a hole-stripe ordered state is responsible for the formation of a pseudogap. Actually, a hole-stripe phase has also been discussed for the manganites to maximize locally the gain of double-exchange energy while keeping globally an insulating behavior.[13] Recent NMR measurements display a nonuniform charge distribution.[14] Therefore, we arrive at the conclusion that holes form a stripe-like state and are mobile within a stripe. Here we stress that an orbital polaron state and a stripe are a natural consequence of gaining a kinetic energy of holes in an insulating background.

We will turn to the distinct shift of the phonon frequencies as a function of temperature observed for the main peaks at 250, 490, and 620 cm^{-1}. It is summarized in Fig. 3 as a function of δ. The experimental spectra are analyzed by a sum of Lorentzian profiles.

First, let us begin with the out-of-phase rotational mode around 250 cm^{-1}. This mode is associated with the tolerance factor of the manganites. That is, it provides direct information about octahedral tiltings and Mn-O-Mn bond angles. With increasing δ the mode softens by 40 cm^{-1}. The large doping dependence is due to the suppression of the static JT distortion as reflected in the structural transition from orthorhombic to rhombohedral phase (see Table I). Further, upon cooling, the 250 cm^{-1} mode first hardens up to T_C and then softens slightly. The magnitude of the hardening decreases as δ increases, for example, from 12 cm^{-1} at δ=0.085 to 4 cm^{-1} at δ=0.125. Since a $d_{3x^2-r^2}/d_{3y^2-r^2}$ orbital ordering is present between T_{JT} and T_C,[9,10] the decrease of the hardening with increasing δ is ascribed to the respective reduction of the $LaMnO_3$-type orbital order, that is, the weakening of the cooperative JT distortion with increasing hole contents. In this regard, the softening by 2–3 cm^{-1} below T_C can be interpreted in terms of the fact that the $LaMnO_3$-type orbital above T_C evolves to the different type of orbital below T_C. Actually, RXS measurements unveil the rearrangement of the orbital ordering through T_C.[9,10]

Next, we will discuss the temperature dependence of the MnO_6 vibrational modes. Upon cooling, the JT mode of the AFI sample at about 490 cm^{-1} shows a slight hardening by 3 cm^{-1} while the breathing mode at about 620 cm^{-1} undergoes a moderate softening by 6 cm^{-1}. For the FMI samples the respective modes exhibit a giant softening by 20–30 cm^{-1} below T_C. As δ increases, the softening becomes enhanced without showing any saturation even at very low temperatures.

As a possible origin we should reflect related lattice anomalies. As pointed out above, the crystal symmetry is reduced around T_{CO} due to the strain caused by the orbital rearrangement. In the respective temperature range lattice parameters undergo an appreciable change.[10] However, these effects are not large enough to explain the observed huge softening of $\Delta\omega/\omega \approx 5\%$. Furthermore, the giant softening is nonexisting in the 250 cm^{-1} mode which is sensitive to lat-

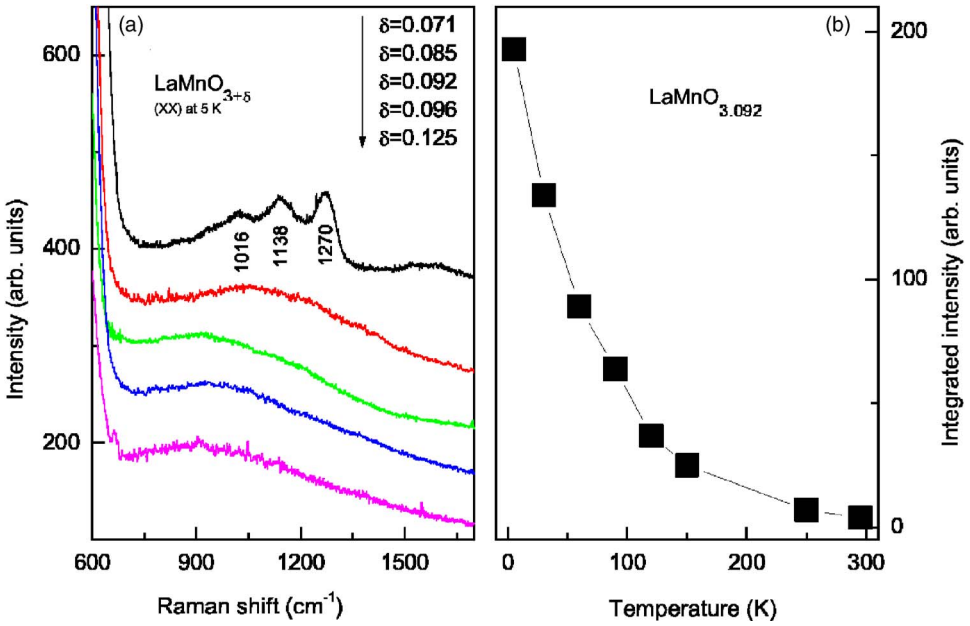

FIG. 4. (Color online) (a) Raman spectra at $T=5$ K in the high-frequency orbiton regime. (b) Temperature evolution of integrated intensity of the maximum at 900 cm^{-1} in the $\delta=0.092$ sample.

tice anomalies. This suggests that the lattice contribution to the softening is minor and cannot account for the magnitude of this effect.

We recall that a giant softening is seen at the breathing mode of the FMI phase of $La_{1-x}Sr_xMnO_3$ and is attributed to orbital-lattice coupling.[12] In this mechanism, the frequency shift of a phonon mode relies on whether the respective ion displacements involve an orbital-ordering pattern. For the manganites the JT and breathing mode are intrinsically coupled to the $LaMnO_3$-type orbital ordering and orbital polaron, respectively.[11] In this light, the giant softening of the JT mode implies that the $LaMnO_3$-type orbital ordering becomes disordered below T_C while the giant softening of the breathing mode is related to the development of orbital polarons. This is compatible with the alternating model consisting of orbital polarons in the hole-rich planes and a $d_{3x^2-r^2}/d_{3y^2-r^2}$ orbital in the hole-poor planes.[12,13] If the orbital rearrangement occurs into the alternating orbital-like state, the phonon frequency will exhibit a steplike temperature dependence. However, the expected saturation is missing, indicating the unstable orbital state. Recent NMR measurements show the instability of the FMI state against the formation of FM nanodomains below 30 K.[14] The irradiation-induced decay of the FMI phase into another insulating phase further supports this.[9] Moreover, the giant softening of the JT mode, which is not pronounced in $La_{1-x}Sr_xMnO_3$,[12] is due to the destabilization of the FMI phase induced by La-site disorder.

Finally, we will address high-frequency Raman spectra of $LaMnO_{3+\delta}$ at 5 K, which are displayed in Fig. 4(a) as a function of δ. The AFI sample shows similar results as $La_{1-x}Sr_xMnO_3$ with respect to frequency, number of modes, and temperature dependence.[25] For the FMI sample of $\delta=0.085$ the three peaks coalesce into a broad maximum near 1100 cm^{-1}. Upon further going to $\delta=0.092$ the broad maximum is shifted to about 950 cm^{-1}. For $\delta=0.092-0.125$ the maximum remains more or less the same. The drastic softening of the broad maximum by 20% through $\delta=0.071-0.125$ is contrasted by the tiny softening of one-phonon scattering of the 490 and 620 cm^{-1} modes by several percentages. Such a behavior can definitely not be understood within pure multiphonon processes. Note that $La_{1-x}Sr_xMnO_3$ shows also a broadened maximum around 1000 cm^{-1} at $x=0.125$.[25] This rules out chemical disorders as its plausible origin. Rather, it pertains to the FMI samples. Since the multiphonon scattering in $LaMnO_3$ is mainly due to the Franck-Condon mechanism via orbiton excitons,[26] the anomalous features of the multiphonon scattering might be closely related to an orbital state.

In the AFI phase the multiphonon scattering is governed by a resonant process induced by an orbital flip of a $d_{3x^2-r^2}/d_{3y^2-r^2}$ orbital ordered state.[26] In this situation, the detailed features of the multiphonon scattering are determined by the underlying orbital-ordering pattern. Upon going through the AF/FMI boundary the $d_{3x^2-r^2}/d_{3y^2-r^2}$ orbitals are rearranged to the alternatinglike orbitals as discussed above. Thus, orbital excitons, which are responsible for the three-peaks feature in the AF phase, will be damped out in the FMI phase. At the same time, gapless orbital excitations will be created due to ferromagnetic spin ordering.[27] As a consequence, the spectral weight of orbital excitations in the FMI phase is expected to shift to lower energy compared to the AFI phase. This explains the unstructured broadening of the multiphonon scattering. Further, its peak energy shifts to lower energy with increasing δ parallel to the enhanced hole mobility and ferromagnetic behavior. The temperature dependence of the integrated intensity of the maximum at $\delta=0.092$ is given in Fig. 4(b). A strong increase of the intensity with decreasing temperature indicates that the intensity is largely determined by the evolution of the charge and orbital states of the FMI phase.

We mention that the observed anomalies of the giant softening of Mn-O modes, the pseudogap state with a Fano antiresonance, and the softening multiphonon scattering through the AF/FMI boundary have a common origin as the orbital fluctuations and significant hole mobilities. This tells

us that the FMI phase is in a delicate balance between the gain of double-exchange energy and the localization of holes.

IV. CONCLUSIONS

In summary, our Raman study of the lightly doped manganites $LaMnO_{3+\delta}$ uncovers a significant hole mobility and an orbital fluctuating state, which form a stripelike state in the FMI state This is demonstrated by the observation of a Fano antiresonance, a giant softening of Mn-O vibration modes, and a broadened multiphonon scattering. Our study hightlights the importance of double-exchange interactions and electronic correlation effects in understanding the occurrence of a ferromagnetic insulating state in the manganites.

ACKNOWLEDGMENTS

We thank J. van den Brink, B. Büchner, M. Braden, G. Khaliulin, D. Khomskii, M. Mostovoy, and M. M. Savosta for useful discussions. This work was supported in part by the DFG and the NATO Collaborative Linkage Grant No. PST.CLG.977766. K.Y.C. is supported by the Grants-in-Aids for Young Scientists (Grant No. 17740209) from JSPS of Japan.

[1] Y. Tokura and N. Nagaosa, Science **288**, 462 (2000).
[2] J. v. d. Brink, G. Khaliullin, and D. Khomskii, *Colossal Magnetoresistive Manganites*, edited by T. Chatterji (Kluwer Academic Publishers, Dordrecht, 2003); cond-mat/0206053 (unpublished).
[3] Y. Endoh, K. Hirota, S. Ishihara, S. Okamoto, Y. Murakami, A. Nishizawa, T. Fukuda, H. Kimura, H. Nojiri, K. Kaneko, and S. Maekawa, Phys. Rev. Lett. **82**, 4328 (1999).
[4] B. Dabrowski, X. Xiong, Z. Bukowski, R. Dybzinski, P. W. Klamut, J. E. Siewenie, O. Chmaissem, J. Shaffer, C. W. Kimball, J. D. Jorgensen, and S. Short, Phys. Rev. B **60**, 7006 (1999).
[5] T. Niemöller, M. v. Zimmermann, J. R. Schneider, S. Uhlenbruck, O. Friedt, Büchner, P. Berthet, L. Pinsad, A. M. de Leon Guevara, and A. Revcolevschi, Eur. Phys. J. B **8**, 5 (1999).
[6] Y. Yamada, O. Hino, S. Nohdo, R. Kanao, T. Inami, and S. Katano, Phys. Rev. Lett. **77**, 904 (1996).
[7] Y. Yamada, J. Suzuki, K. Oikawa, S. Katano, and J. A. Fernandez-Baca, Phys. Rev. B **62**, 11600 (2000).
[8] R. Klingeler, J. Geck, R. Gross, L. Pinsard-Gaudart, A. Revcolevschi, S. Uhlenbruck, and B. Büchner, Phys. Rev. B **65**, 174404 (2002).
[9] J. Geck, P. Wochner, D. Bruns, B. Büchner, U. Gebhardt, S. Kiele, P. Reutler, and A. Revcolevschi, Phys. Rev. B **69**, 104413 (2004).
[10] J. Geck, P. Wochner, S. Kiele, R. Klingeler, A. Revcolevschi, M. v. Zimmermann, B. Büchner, and P. Reutler, New J. Phys. **6**, 152 (2004).
[11] R. Kilian and G. Khaliullin, Phys. Rev. B **60**, 13458 (1999).
[12] K.-Y. Choi, P. Lemmens, T. Sahaouri, G. Güntherodt, Yu. G. Pashkevich, V. P. Gnezdilov, P. Reutler, L. Pinsard-Gaudart, B. Büchner, and A. Revcolevschi, Phys. Rev. B **71**, 174402 (2005).
[13] T. Mizokawa, D. I. Khomskii, and G. A. Sawatzky, Phys. Rev. B **61**, R3776 (2000).
[14] G. Papavassiliou, M. Pissas, G. Diamantopoulos, M. Belesi, M. Fardis, D. Stamopoulos, A. G. Kontos, M. Hennion, J. Dolinsek, J.-Ph. Ansermet, and C. Dimitropoulos, Phys. Rev. Lett. **96**, 097201 (2006).
[15] C. Ritter, M. R. Ibarra, J. M. De Teresa, P. A. Algarabel, C. Marquina, J. Blasco, J. Garcia, S. Oseroff, and S. W. Cheong, Phys. Rev. B **56**, 8902 (1997).
[16] F. Prado, R. D. Sanchez, A. Caneiro, M. T. Causa, and M. Tovar, J. Solid State Chem. **146**, 418 (1999).
[17] S. N. Barilo, V. I. Gatal'skaya, S. V. Shiryaev, G. L. Bychkov, L. A. Kurochkin, S. N. Ustinovich, R. Szymczak, M. Baran, and B. Drzymanska, Phys. Solid State **45**, 146 (2003).
[18] W. H. McCarrol, K. V. Ramanujachary, and M. Greenblatt, J. Solid State Chem. **130**, 327 (1997).
[19] J. Geck (private communication).
[20] M. N. Iliev, M. V. Abrashev, H.-G. Lee, V. N. Popov, Y. Y. Sun, C. Thomsen, R. L. Meng, and C. W. Chu, Phys. Rev. B **57**, 2872 (1998).
[21] T. Mizokawa, D. I. Khomskii, and G. A. Sawatzky Phys. Rev. B **60**, 7309 (1999).
[22] K.-Y. Choi, P. Lemmens, G. Güntherodt, M. Pattabiraman, G. Rangarajan, V. P. Gnezdilov, G. Balakrishnan, D. McK. Paul, and M. R. Lees, J. Phys.: Condens. Matter **15**, 3333 (2003).
[23] N. Mannella, W. L. Yang, X. J. Zhou, H. Zheng, J. F. Mitchell, J. Zaanen, T. P. Devereaux, N. Nagaosa, Z. Hussain, and Z.-X. Shen, Nature (London) **438**, 474 (2005).
[24] V. P. Gnezdilov, A. V. Yeremenko, Yu. G. Pashkevich, P. Lemmens, G. Güntherodt, J. M. Tranquada, D. J. Buttrey, and K. Nakajima, Low Temp. Phys. **28**, 510 (2002).
[25] K.-Y. Choi, P. Lemmens, G. Güntherodt, Yu. G. Pashkevich, V. P. Gnezdilov, P. Reutler, L. Pinsard-Gaudart, B. Büchner, and A. Revcolevschi, Phys. Rev. B **72**, 024301 (2005).
[26] R. Krüger, B. Schulz, S. Naler, R. Rauer, D. Budelmann, J. Bäckström, K. H. Kim, S.-W. Cheong, V. Perebeinos, and M. Rübhausen, Phys. Rev. Lett. **92**, 097203 (2004).
[27] J. van den Brink, P. Horsch, F. Mack, and A. M. Oles, Phys. Rev. B **59**, 6795 (1999).